Atatürk Üniv Diş Hek Fak Derg (*J Dent Fac Atatürk Uni*)
Cilt:30, Sayı:1, Yıl: 2020, Sayfa: 12-19

Araştırma/ Research Article

EVALUATION OF INTRAORAL ORTHODONTIC BRACKETS' EFFECTS ON MAGNETIC RESONANCE IMAGING –A CADAVERIC STUDY AT 3 TESLA

İNTRAORAL ORTODONTIK BRAKETLERIN MANYETIK REZONANS GÖRÜNTÜLER ÜZERINE ETKILERININ DEĞERLENDIRILMESI - 3 TESLA'DA BIR KADAVRA ÇALIŞMASI

Doç. Dr. Mehmet Hakan KURT [*] **Doç. Dr. Mehmet Eray KOLSUZ**[*]
Doç. Dr. Ulaş ÖZ[**] **Doç. Dr. İsmail Hakan AVSEVER**[***]
Doç. Dr. Tuğrul ÖRMECİ[****] **Prof. Dr. Bayram Ufuk ŞAKUL**[*****]
Prof. Dr. Kaan ORHAN[*]

Makale Kodu/Article code: 4058
Makale Gönderilme tarihi: 03.05.2019
Kabul Tarihi: 21.11.2019
DOI : *10.17567/ataunidfd.649475*

Mehmet Hakan Kurt: *ORCID ID:* 0000-0001-8312-5674
Mehmet Eray Kolsuz: *ORCID ID:* 0000-0001-8872-1897
Ulaş Öz: *ORCID ID:* 0000-0002-5203-577X
İsmail Hakan Avsever: ORCID ID: 0000-0002-2972-2547
Tuğrul Örmeci: *ORCID ID:* 0000-0001-8532-4917
Bayram Ufuk Şakul: *ORCID ID:* 0000-0002-5539-2342
Kaan Orhan: *ORCID ID:* 0000-0001-6768-0176

ABSTRACT
Aim: Artifacts caused by orthodontic attachments limit the diagnostic value and lead to the removal of these appliances before magnetic resonance imaging. The magnet strength can influence the artifact size due to orthodontic appliances. Moreover, new (ceramic/clear) brackets have not evaluated. Hence, the purpose of this study was to quantitively evaluated the artifacts and heat due to different intra-oral appliances on Magnetic Resonance Imaging.
Material and Method: The study based on a fresh cadaver head. Three intra-oral orthodontic appliances (i.e. metal/metal-ceramic and ceramic clear brackets) together with metallic wires were scanned in a 3 Tesla magnetic resonance device (3-Tesla Philips Achieva) using different sequences. Artifact areas were determined and the temperature evaluated before and after MRI scanning.
Results: The smallest artifact was produced by Ceramic (clear) Brackets scanned in a 3D FLAIR sequence with a dimension of 9,1 mm on sagittal images. The steel-containing orthodontic devices were associated with radius artifacts ranging from 34,45 mm to 47,35 mm. No significant difference found for heat before and after scanning ($p \leq 0.05$).
Conclusion: Consequently, the choice of intra-oral orthodontic appliances and awareness of the composition of appliances together with magnetic interference is crucial for head and neck magnetic resonance scanning that has to take into consideration by both orthodontic consultants and the radiologists.
Key Words: Magnetic Resonance Imaging, Heat, Artifact, Orthodontics, Ceramic Brackets

ÖZ
Amaç: Ortodontik aygıtların neden olduğu artefaktlar teşhis değerini kısıtlamaktadır. Manyetik rezonans görüntülemeden önce bu aygıtların çıkarılması gerekmektedir. Bunula birlikte manyetik kuvvetin büyüklüğü ortodontik aygıtlardan dolayı oluşan artefaktalrın boyutunu etkilemektedir. Bugüne kadar, tamamen seramik olan yeni braketlerin oluşturabileceği artefakt boyutu detaylı bir şekilde değerlendirilmemiştir. Bu çalışmanın amacı, farklı ağız içi ortodontik braketlerin manyetik rezonans görüntüleme esnasındaki oluşturdukları artefaktları ve oluşan ısıyı nicel olarak değerlendirmektir.
Gereç ve Yöntem: Çalışma taze bir kadavra kafası ile yapıldı. Üç farklı ortodontik braket (metal / metal-seramik ve seramik şeffaf braketler) dişlere yapıştırıldıktan sonra farklı sekanslar kullanılarak 3 Tesla manyetik rezonans cihazında (3 Tesla Philips Achieva) tarandı. Oluşan artefakt alanları tespit edildi ve MRI taramasından önce ve sonra sıcaklık değişimleri de değerlendirildi.
Bulgular: En küçük artefakt çapı, sagittal görüntülerde 9,1 mm boyutlarındaydı. Bu artefakt 3D FLAIR sekansında taranan seramik braketler ile oluştu. Çelik içeren ortodontik braketler 34,45 mm ila 47,35 mm arasında değişen artefakt çaplarına sahipti. Tarama öncesi ve sonrası ısı açısından anlamlı bir fark bulunmadı ($p \leq 0.05$).
Sonuç: Baş ve boyun manyetik rezonans taraması için ağız içi ortodontik braketlerin seçimi ile bunların içeriklerinin ve bu aygıtların manyetik alandan nasıl etkilendiğinin bilinmesi hem ortodontistlerin hem de radyologların göz önünde bulundurması gereken bir durumdur.
Anahtar Kelimeler: Manyetik Rezonans Görüntüleme, Isı, Artefakt, Ortodonti, Seramik Braket

[*] Dentomaxillofacial Radiology, Faculty of Dentistry, Ankara University, Ankara, Turkey
[**] Orthodontics, Faculty of Dentistry, Near East University, Lefkosa, Mersin 10, Turkey
[***] Dentomaxillofacial Radiology, Faculty of Gulhane Dentistry, Health Sciences University, Ankara, Turkey
[****] Medipol University, Radiology, Faculty of Medicine, Istanbul, Turkey
[*****] Anatomy, Faculty of Medicine, Medipol University, Istanbul, Turkey

Kaynakça Bilgisi: Kurt MH, Kolsuz ME, Öz U, Avsever İ, Tuğrul Ö, Şakul BU. İntraoral Ortodontik Braketlerin Manyetik Rezonans Görüntüler Üzerine Etkilerinin Değerlendirilmesi - 3 Tesla'da Bir Kadavra Çalışması Atatürk Üniv Diş Hek Fak Derg 2020; 30: 12-19.
Citation Information: *Kurt MH, Kolsuz ME, Oz U, AvseverI, Tugrul O, Sakul BU. Evaluation Of Intraoral Orthodontic Brackets' Effects On Magnetic Resonance Imaging –A Cadaveric Study At 3 Tesla. J Dent Fac Atatürk Uni 2020; 30: 12-19.*

INTRODUCTION

Magnetic resonance imaging (MRI) is a widely used diagnostic imaging technique in which tissue images acquired via magnetic resonance (MR) of atomic nuclei by using a static field and a magnetic field that changes with time[1]. It regarded as an ideal diagnostic tool for the imaging of anatomical structures in the brain and craniofacial areas due to the presence of high tissue contrast. While high-resolution MRI plays an important role in the clinical anatomic imaging of the pituitary gland[2,3], dynamic contrast improvement techniques are beneficial for the diagnosis of pituitary and sellar lesions[4]. Today, MRI has become the most efficient imaging method for evaluating temporomandibular joints (TMJ)[5,6]. In a non-invasive manner with no ionizing radiation, it can create images in different planes and resolutions. Therefore, it is highly suitable for the pediatric population, including the clinical assessment of cleft palate anatomy[7,8].

The 3-Tesla MRI is now widely used in clinical imaging as it provides a high signal-noise ratio and high spatial resolution[9]. Its use has steadily increased among pediatricians to overcome the challenges presented by pediatric imaging cases[10]. High spatial resolution is particularly useful for the imaging of young children, especially for smaller structures such as the inner ear, brachial plexus, biliary system, and vascular system[9,10].

When placed into a magnetic field, all materials are magnetized to some extent, depending on the magnetic sensitivity of the particular material[11,12]. The materials used in dentistry, including metallic restorations, could create serious artifacts in maxillofacial imaging according to their magnetizability. Metallic materials can classified in terms of their magnetic sensitivity as ferromagnetic, paramagnetic, or diamagnetic[13-15].

Fixed orthodontic devices consist of several materials, such as stainless steel, titanium or ceramics. Many studies have reported unfavorable effects of these devices on MR images during the process of head and neck imaging, especially for the soft palate and velopharyngeal wall[16-20]. Moreover, fixed devices can removed in patients receiving orthodontic therapy when an MRI performed. Consequently, the detachment of orthodontic devices is a dissatisfactory situation for these patients, who subsequently faced with costly and long-term treatment protocols. Due to the poor diagnostic quality of MRI that caused by orthodontic devices via their artifacts, physicians should weigh and balance its benefit/risk ratio or appropriately combine orthodontic devices for those patients who will require MRI[21-22].

To the best of the authors' knowledge, there is no studies that have investigated the radii of artifacts and temperature changes, which created by different orthodontic devices on the images in all three planes. It also did not studied acquired with different imaging sequences (Turbo Spin Echo (TSE), Spin Echo (SE), Diffusion Weight Imaging (DWI b0, b500, b1000), Three-Dimensional Fluid Attenuated Inversion Recovery (3D FLAIR) and Diffusion Weight Imaging with Sensitivity Encoding (DWI-SENSE)) in an ex-vivo set-up. Hence, the purpose of this study was to quantitively evaluated the artifacts and heat due to different intra-oral brackets on MRI.

METHOD AND MATERIALS

This *ex-vivo* study conducted in accordance with the principles of the Declaration of Helsinki. Three different orthodontic brackets Damon Q made with steel (Ormco, California, USA), Damon 3 made with steel-ceramic (Ormco, California, USA), Damon Clear made with ceramic (Ormco, California, USA) were adhered to human cadaveric teeth via routinely used materials. A total of 10 brackets were applied for each bracket materials onto the maxillary teeth (from right second premolar to the left second premolar) and tubes were attached to first molars. Afterward, using head and neuromuscular coil (8ch phased-array coil) to obtain MR images placed the head of the cadaver into a 3-T MRI device (3-Tesla Philips Achieva). The structural compositions of the examined brackets presented in *Table 1*.

For each model, MR images were obtained at 3-mm sections in different planes by using 3D FLAIR (sagittal), T2W-TSE (axial and coronal), T1W-SE (axial), T1W-IR-TSE (coronal), DWI b0 (axial), b500 (axial), b1000 (axial), and DWI with SENSE (axial) sequences. MR parameters shown in Table 2. The temperature gradients of all teeth were measured at a 3-cm distance from the tooth surface before and immediately after the MRI scanning with a dual laser infrared thermometer (Extech 42511, Boston, USA) (Figure 1).

MR images were assessed with 3D Synapse software (Fuji Film, Japan) and the measurements were performed on a 21.3-inch flat panel color active matrix TFT medical display (NEC MultiSync MD215MG, München, Germany) with a resolution of 2048 x 2560 at 75 Hz and 0.17-mm dot pitch operated at 11.9 bits. All artifacts were assessed at sagittal, coronal, and axial sequences with three different orthodontic brackets (steel, steel-ceramic, and ceramic) (Figure 2-4). The radius of the artifact defined as the distance from the center of the image to the last point in which the signal acquired. A single observer (KO) evaluated all measurements and evaluations of each measurement repeated 2 months after the first measurement. The mean of the measured values corresponded to the final length of the radius.

Observer reliability and statistical methods

Statistical analyses done using the IBM SPSS version 20 (SPSS Inc. Chicago, Illinois, USA) statistics package program. Descriptive statistics presented as the mean, ±standard deviation, and median. Intra-observer validation measures also conducted. To assess intra-observer reliability, the intraclass correlation coefficient (ICC) used for repeated measurements.

A paired t-test used when the normal distribution assumptions made otherwise Wilcoxon signed-rank test used to determine differences between pre and post-heating in each of three heating measurements for different materials. A p-value less than 0.05 considered statistically significant ($p \leq 0.05$).

Table 1. Contents of the orthodontic brackets and tubes

Product:	**Alloy**	**Chemical composition (wt. %) (Note: Single values are maximum values unless otherwise indicated)**							**Magnetic**
Damon 3 (Ormco, California, USA)	AISI Type	Carbon C	Manganese Mn	Silicone Si	Chromium Cr	Nickel Ni	Other	Iron Fe	Yes
Damon Q (Ormco, California, USA)	17 - 4 PH Stainless steel	0.07	0.5	1.00	15.0 - 17.5	3.0 -5.0	P 0.04 S 0.03 Cu 3.0-5.0 Nb 0.15-0.45 Co 0.5 Mo 0.2	Balance	Yes
Damon Clear (Ormco, California, USA)	Polycrystalline Alumina (PCA) + NiTi Locking Pin*								

Table 2. Technical parameters for 3Tesla MRI scanning

Parameters	**T_2W-TSE (axial)**	**T_2W-TSE (coronal**	**T_1W-SE (axial)**	**T_1W-IR-TSE (coronal)**	**3D FLAIR (sagittal)**	**DWI (b=0) (axial)**	**DWI (b=500) (axial)**	**DWI (b=1000) (axial)**	**DWI with SENSE(b=1000) (axial)**
FOV (mm)	**481x836**	**141x246**	**420x656**	**256x256**	**256x256**	**249x434**	**249x435**	**249x436**	**249x436**
Voxel size (mm)	**0.7x0.5x2.4**	**0.7x0.5x4**	**0.7x0.5x3**	**0.7x0.5x3**	**1.2x1.2x1.2**	**0.375x0.375x0.375**	**0.375x0.375x0.375**	**0.375x0.375x0.375**	**0.375x0.375x0.375**
Slice Thickness (mm)	**5**	**5**	**5**	**5**	**12**	**5**	**5**	**5**	**5**
TE (ms)	**80**	**182**	**10**	**15**	**182**	**85**	**85**	**85**	**85**
TR (ms)	**3000**	**4800**	**644**	**4780**	**4800**	**3120**	**3120**	**3120**	**3120**
Scan time (min:s)	**02:24**	**02:28**	**08:29**	**08:25**	**03:19**	**03:18**	**03:18**	**03:18**	**03:18**
Flip Angle	**90-120^0**	**90-120^0**	**90-120^0**	**90-120^0**	**10^0**	**70^0**	**70^0**	**70^0**	**70^0**
B1 ms (μT)	**1.8**	**1.8**	**2**	**2**	**0.6**	**0.7**	**0.7**	**0.7**	**0.7**
ETL	**4**	**4**	**4**	**4**	**4**	**4**	**48**	**48**	**48**

FOV, Field of View; TE, Echo Time; TR, Repetition Time; T2W, T2 Weighted; T1W, T1 Weighted; TSE, Turbo Spin Echo; SE, Spin Echo; 3D FLAIR, 3 Dimensional Fluid-attenuated Inversion Recovery; IR, Inversion Recovery; DWI, Diffusion Weighted Imaging; SENSE, Such as Sensitivity Encoding; ETL, Echo Train Length

Figure 1. a, Metal and b, ceramic bracket application to cadaver's maxillary teeth; c, direct temperature measurement with dual laser infrared thermometer; d, MRI application of the cadaver's head

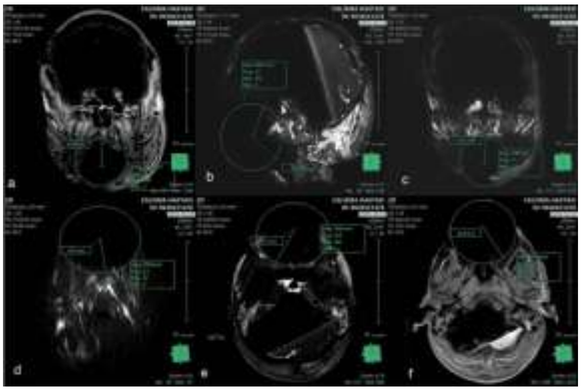

Figure 2. Artifact measurements of steel brackets. a, T_1 coronal plane; b, 3D flair sagittal plane; c, T_2 coronal plane; d, DWI axial plane; e, T_2 axial plane; f, T_1 axial plane

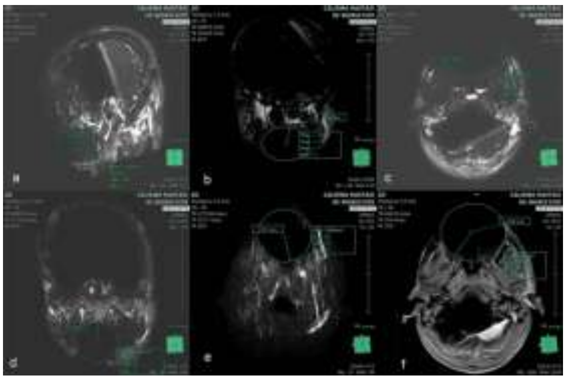

Figure 3. Artifact measurements of steel-ceramic brackets. a, 3D flair sagittal plane; b, T_2 coronal plane; c, T_2 axial plane; d, T_1 coronal plane; e, DWI sense axial plane; f, T_1 axial plane

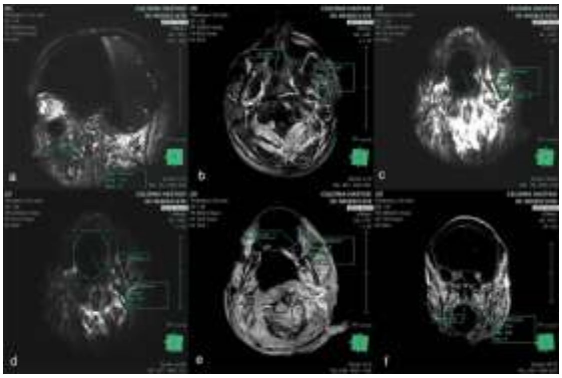

Figure 4. Artifact measurements of ceramic brackets. a, 3D flair sagittal plane; b, T_2 axial plane; c, DWI axial plane; d, DWI sense axial plane; e, T_1 axial plane; f, T_1 coronal plane

RESULTS

All measurements found to be highly reproducible. Overall intra-observer consistency was rated at 0.998 (0.995-0.999) between the two measurements.

The artifact diameters presented in table 3. The smallest artifact radius occurred in the 3D FLAIR sequence with a dimension of 9,1 mm on sagittal images with ceramic brackets. The largest artifact diameter was obtained in the DWI (b=1000) sequence on the axial plane. Steel brackets caused this artifact diameter, measured as 47.3 mm. In general, steel brackets produced the most artifact diameter. Moreover, the artifact diameter related to the MR scan sequences and scanning planes.

Temperature measurements before the MRI yielded were detected for all 12 teeth to be at a mean of 19,09 °C (± 0,07). On the other hand, the highest temperature was measured as 20,55 °C (± 0,10) after MRI scanning in the T1W-IR-TSE sequence for steel brackets. The lowest temperature was measured as 19,07 (± 0,12) in the T2W-TSE sequence for ceramic brackets. All of the brackets were increased the temperatures after MRI scanning. However, these temperature alterations were statistically non-significant ($p>0.05$) (Table 4).

DISCUSSION

Dental implants, orthodontic brackets, and wires, metal-supported fixed and removable restorations, etc. are widely used in dentistry.

Table 3. Artifact diameters according to brackets in the studied MR sequences

	Steel				Steel-Ceramic				Ceramic			
	1st evaluation	2nd evaluation	Mean	±Sd	1st evaluation	2nd evaluation	Mean	±Sd	1st evaluation	2nd evaluation	Mean	±Sd
T2W-TSE (axial)	45,7	48,8	47,25	2,19	34,2	35,4	34,8	,84	13,8	12,5	13,15	,91
T2W-TSE (coronal)	37,7	37,8	37,75	,07	24,9	25,6	25,25	,49	14,5	14,2	14,35	,21
T1W-SE (axial)	44,4	43,8	44,1	,42	35,9	35,8	35,85	,07	29	28,7	28,85	,21
T1W-IR-TSE (coronal)	34,3	34,6	34,45	,21	27,6	28,4	28	,56	22,5	21,5	22	,70
3D FLAIR (sagittal)	43,4	44,5	43,95	,77	36,2	36,4	36,3	,14	9	9,2	9,1	,14
DWI (b=0) (axial)	42,5	42,8	42,65	,21	38,7	39,4	39,05	,49	28,4	27,3	27,85	,77
DWI (b=500) (axial)	46,8	45,9	46,35	,63	40,3	40,5	40,4	,14	30,2	30	30,1	,14
DWI (b=1000) (axial)	45,5	45,1	45,3	,28	32,8	31,6	32,2	,84	30,2	30	30,1	,14
DWI with SENSE (b=1000) (axial)	47,3	47,4	47,35	,07	35,9	36,2	36,05	,21	30,8	28,6	28,7	1,55

Table 4. The results of the temperature changes before and after MRI scanning

	Before Scanning				After Scanning														
	N	Mean	± Sd	Med	Steel					Steel-Ceramic					Ceramic				
					N	Mean	± Sd	Med	p-value[a]	N	Mean	± Sd	Med	p-value[a]	N	Mean	± Sd	Med	p-value[a]
T2W-TSE (axial)	12	19,09	,10	19,10	12	19,71	,11	19,70	>0,05	12	19,34	,09	19,30	>0,05	12	19,07	,12	19,05	>0,05
T2W-TSE (coronal)					12	19,50	,07	20	>0,05	12	19,73	,08	19,70	>0,05	12	19,49	,10	19,50	>0,05
T1W-SE (axial)					12	19,97	,06	20	>0,05	12	19,70	,08	19,70	>0,05	12	19,49	0,9	19,50	>0,05
T1W-IR-TSE (coronal)					12	20,55	,10	20,50	>0,05	12	20,25	,11	20,25	>0,05	12	20,01	,09	20	>0,05
3D FLAIR (sagittal)					12	20,25	,09	20,30	>0,05	12	20,01	,11	20	>0,05	12	19,71	,10	19,70	>0,05
DWI (b=0) (axial)					12	19,56	,13	19,60	>0,05	12	19,24	,18	19,30	>0,05	12	19,10	,10	19,11	>0,05
DWI (b=500) (axial)					12	19,68	,07	19,70	>0,05	12	19,35	,10	19,30	>0,05	12	19,13	,08	19,11	>0,05
DWI (b=1000) (axial)					12	19,80	,07	19,80	>0,05	12	19,43	,09	19,40	>0,05	12	19,19	,07	19,20	>0,05
DWI with SENSE (b=1000) (axial)					12	19,26	,08	19,80	>0,05	12	19,23	,10	19,20	>0,05	12	19,15	,10	19,16	>0,05

[a] *p*-values belong to paired t-test and Wilcoxon signed-rank test

Magnetic field interactions of metal objects, which used in dentistry, should known. Anamnesis should taken for metallic objects, which affected by the magnetic field in the patient's body. It will reduce patient risk during magnetic resonance imaging [23]. There are a limited number of studies have investigated the effects of orthodontic brackets on MR images in which, the effects of metal structures have been examined with metal-containing prosthetic materials [24-28]. Available studies evaluating orthodontic devices have not been comprehensive or comparable in terms of materials. Furthermore, many of these studies were designed as in vitro experiments, failing to reflect real clinical conditions[16,29,30]. To overcome this deficiency, cadavers wused in this study to provide a better model for clinical settings.

Previous studies have used 1.5T or 3-T MR devices, largely with T1 or T2 sequences[31-35]. However, advance MRI sequences have not been determined for this kind of experimental set-ups especially rapid imaging with either multi-planar DWI or single-shot fast spin-echo (SSFSE) sequences that were routinely used to provide a quick assessment of major strokes and ventricular dimensions. It particularly emphasized that a 3-D dataset with a high spatial resolution needed to generate for whole-brain scanning where pediatric patients are concerned. Sagittal T1-weighed and T2-weighted or 3D FLAIR sequences recommended to distinguish gray and white matters and to evaluate white matter abnormalities during overall brain assessment, including midline structures. Moreover, 3-D gradient T1 or T2/FLAIR-weighed images recommended assessing the brain anatomy[36]. However, these sequences are slightly longer than conventional T1 and T2 sequences, which may prone to motion artifact. Thus, evaluation of these sequences is crucial especially with intra-oral appliances. Hence, in the present study, MR images obtained by placing the head of the cadaver into a 3-T MRI device by using TSE, FSE, DWI b0, b500, b1000 sequences. Zachriat et al.[34] reported a study with ceramic and steel brackets in a 1.5-T MR device. They reported the image artifacts with diameters of 1.1 for ceramic and

7.4 cm for steel and 1.3 cm for Ni-Ti orthodontic appliances on coronal and sagittal planes using a cuboidal polymethylmethacrylate phantom, respectively. Additionally, they found that it reduced by 32.7% with the use of the artifact-minimizing WARP sequence. The investigators showed that brain imaging with TSE sequence was not associated with artifacts, except in the nasal cavity, and that cervical vertebra imaging with TSE sequence. They further reported that the GRE sequence caused more acceptable artifacts than TSE sequence.

Beau et al.[31] determined that artifact ratios emerged secondary to different orthodontic brackets during imaging performed with a 1.5-T MRI device. The authors reported that stainless steel brackets were always associated with artifacts (100%), while titanium, steel-slot ceramic, and stainless steel enhancing wires caused artifacts by 20.0%, 16.7%, and 86.5%, respectively.

Wylezinska et al.[35] evaluated the effects of orthodontic devices on anatomical structures in the craniofacial area including the soft palate, velopharyngeal wall, temporomandibular joint, and pituitary gland where they used real-time speech sequence with a 1.5-T MRI device. Accordingly, the metallic orthodontic devices exhibited distinguishable effects on image quality. The most prominent effects were observed with stainless steel brackets and steel arches combined with stainless steel molar bands. MRIs with the latter device showed a significantly poor diagnostic quality in the speech and palate images. It further reported that the pituitary gland and temporomandibular joint could not visualized with these devices, whereas the metal-free, Ni/Cr supported, or Ni/Ti alloyed orthodontic devices were associated with minimal problems in the image quality.

In the present study, the highest radii of the image artifacts were measured in millimeters and were found to be 43,95 mm, 36,4 mm, and 9,1 mm of artifacts at the sagittal plane by steel, steel-ceramic, and ceramic brackets, respectively. On the other hand, these brackets were associated with 47,35 mm, 40,4 mm, and 30,1 mm artifacts at the axial plane, respectively. In coronal sequences, the radii of the artifacts were 37,75 mm, 28 mm, and 22 mm, respectively. Therefore, different radii of artifacts revealed for all the three planes. The smallest artifact originated from ceramic brackets at the axial plane of 3D FLAIR sequence, whereas steel brackets at the axial plane of DWI with SENSE b1000 sequence produced the largest artifact.

No studies have been conducted where the thermal effect of the magnetic field on orthodontic devices was investigated by measuring the temperature directly from the teeth surface; instead, they have utilized infrared thermometers or fiber optic thermometers which were immersed into the saline-containing solutions with the samples to detect temperature alteration[32,33]. Hasegawa et al.[32] reported that orthodontic devices caused a 2.61 °C temperature elevation. On the other hand, Gorgulu et al.[33], in their study with a 3-T MRI device, reported that no tested materials had excessive warming, with a maximal temperature change of 3.4 °C observed in the T1-weighed axial images. In the present study, a 0,02 °C to 1,46 °C temperature gradient was found between the before and after MRI values which were not statistically significant. The authors believe that this low-temperature gradient, which is inconsistent with other studies, can attributed to the performance of the measurement of the temperature directly from the surface of the teeth. It believed that the saline solutions that used in previous studies might also influenced by the magnetic field, escalating the current temperature.

Limitations of the study

Considering that orthodontic patients tend to belong to the pediatric population and MRI requires immobilization during the procedure, the use of a cadaver model completely eradicated motion artifacts that would arise during real-life imaging procedures, which regarded as a limitation of the present study. Moreover, the authors did not evaluate the archwire, since it could be easily detached before MRI. Furthermore, several factors such as the absence of blood flow and no preservation of pulpal tissue vitality by teeth in the cadaveric model might have contributed to the observation of the low-temperature gradient. Nevertheless, this needs to verify by further clinical trials.

The present study shows that orthodontic devices cause a slight but clinically non-harmful temperature elevation in teeth and the surrounding tissues; hence, the possibility of thermal increase during MRI could ignored without necessitating the removal of the orthodontic devices before the procedure. Furthermore, considering the sizes of the artifacts associated with steel and ceramic brackets, it can suggested that it is reasonable to prefer ceramic brackets in a patient who requires a routine head and neck MRI scanning; alternatively, if this is not possible, the steel brackets should be detached before commencing the MRI procedures.

In conclusion, not only radiologists but also orthodontists or dentists need to be aware of the types and compositions of the devices before the initiation of long-term orthodontic permanent treatment that requires follow-up with head and neck MRI.

Acknowledgments

Near East University Scientific Project Coordination Unit with the project number of CE060-2015 funded this project.

NOT: Çalışmada herhangi bir yazar, kurum ya da kuruluş ile çıkar çatışması içerisinde bulunmamaktadır. Makale daha önce hiçbir yerde yayınlanmamış ve yayınlanmak üzere işlem görmemektedir

REFERENCES

1. American Society for Testing and Materials (ASTM) International. Standard F2182-02a: Standard Test Method for Measurement of Radio Frequency Induced Heating Near Passive Implants During Magnetic Resonance Imaging. West Conshohocken, PA: ASTM International; 2002.
2. Elster A, Chen M, Williams D, Key L. Pituitary gland: MR imaging of physiologic hypertrophy in adolescence. Radiology 1990; 174: 681–5.
3. Marro B, Zouaoui A, Shel M, Rudish A. MRI of pituitary adenomas on acromegaly. Neuroradiology 1997; 39: 394–9.
4. Smallridge RC, Czervionke LF, Fellows DW, Bernet VJ. Cortotropin- and thyrotropin-secreting pituitary microadenomas: detection by magnetic resonance imaging. Mayo Clin Proc 2000; 75: 521–8.
5. Larheim TA. Role of magnetic resonance imaging in the clinical diagnosis of temporomandibular joint. Cells Tissues Organs 2005; 180: 6–21.
6. Emshoff R, Brandlmaier I, Gerhard S, Strobi H, Bertram S. Magnetic resonance imaging predictors of temporomandibular joint pain. J Am Dent Assoc 2003; 134: 705–14.
7. Raanan A, McDonough M, Corbin AM, et al. Linear dimensions of the upper airway structure during development, assessment by magnetic resonance imaging. Am J Respir Crit Care Med 2002; 165: 117–22.
8. Perry LJ, Kuehen DP, Sutton BP. Morphology of the levator veli palatini muscle using magnetic resonance imaging. Cleft Palate Craniofac J 20013; 50: 64–7.
9. Kuhl CK, Traber F, Schild HH. Whole-body high-field-strength (3.0-T) MR imaging in clinical practice. Part I. Technical considerations and clinical applications. Radiology 2008; 246: 675–96.
10. Dagia C, Ditchfield M. 3T MRI in paediatrics: challenges and clinical applications. Eur J Radiol 2008; 68: 309–19.
11. Elison JM, Leggitt VL, Thomson M, Oyoyo U, Wycliffee ND. Influence of common orthodontic appliances on the diagnostic quality of cranial magnetic resonance images. Am J Orthod Dentofacial Orthop 2008; 134: 563-72.
12. Harris TMJ, Faridrad MR, Dickson JAS. The benefits of aesthetic orthodontic brackets in patients requiring multiple MRI scanning. J Orthod 2006; 33: 90-4.
13. Shellock FG, Kanal E. Aneurysm clips: evaluation of MR imaging artifacts at 1.5 T. Radiology 1998; 209: 563-6.
14. Destine D, Mizutani H, Igarashi Y. Metallic artifacts in MRI caused by dental alloys and magnetic keeper. Nihon Hotetsu Shika Gakkai Zasshi 2008; 52: 205-10.
15. Shafiei F, Honda E, Takahashi H, Sasaki T. Artifacts from dental casting alloys in magnetic resonance imaging. J Dent Res 2003; 82: 602-606.
16. Okano Y, Yamashiro M, Kaneda T, Kasai K. Magnetic resonance imaging diagnosis of thetemporomandibular joint in patients with orthodontic appliances. Oral Surg Oral Med Oral Pathol Oral Radiol Endod 2003; 95: 255-63.
17. Kemper J, Klocke A, Kahl-Nieke B, Adam G. Orthodontic Brackets in High Field Magnetic Resonance Tomography: Experimental assessment of magnetic attraction and rotational forces at 3 Tesla. RöFo 2005; 177: 1691-8. [In German].
18. Patel A, Bhavra GS, O'Neill JR. MRI scanning and orthodontics. J Orthod. 2006; 33: 246-9.
19. Hatch J, Deahl TS, Matteson SR. CAT of the month: Remove metallic orthodontic appliances prior to MRI imaging. Tex Dent J 2014; 131: 26.
20. Kajan ZD, Khademi J, Alizadeh A, Hemmaty YB, Roushan ZA. A comparative study of metal artifacts from common metal orthodontic brackets in magnetic resonance imaging. Imaging Sci Dent 2015; 45: 159-68.

21. Vandevenne JE, Vanhoenacker FM, Parizel PM, Butts PK, Lang RK. Reduction of metal artefacts in musculoskeletal MR imaging. JBR-BTR 2007; 90: 345–9.
22. Eggers G, Rieker M, Kress B, Fiebach J, Dickhaus H, Hassfeld S. Artefacts in magnetic resonance imaging caused by dental material. MAGMA 2005; 18: 103-11.
23. Karaman T, Eşer B, Güven S, Yıldırım TT. Magnetic resonance imaging in dentistry and its effect on dental materials. J Dent Fac Atatürk Uni 2018; 28: 271-6.
24. New PF, Rosen BR, Brady TJ, et al. Potential hazards and artifacts of ferromagnetic and nonferromagnetic surgical and dental materials and devices in nuclear magnetic resonance imaging. Radiology 1983; 147: 139–8.
25. Hinshaw DB, Jr Holshouser BA, Engstrom HI, Tjan AH, Christiansen EL, Catelli WF. Dental material artifacts on MR images. Radiology 1988; 166: 777–9.
26. Lissac M, Coudert JL, Briguet A, Amiel M. Disturbances caused by dental materials in magnetic resonance imaging. Int Dent J 1992; 42: 229–33.
27. Masumi S, Arita M, Morikawa M, Toyoda S. Effect of dental metals on magnetic resonance imaging (MRI). J Oral Rehabil 1993; 20: 97–106.
28. Starcuk Z, Bartusek K, Hubalkova H. Evaluation of MRI artifacts caused by metallic dental implants and classification of the dental materials in use. Meas Sci Rev 2006; 6: 24–7.
29. Sadowsky PL, Bernreuter W, Lakshminarayanan AV, Kenney P. Orthodontic appliances and magnetic resonance imaging of the brain and temporomandibular joint. Angle Orthod 1988; 58: 9–20.
30. Elison MJ, Leroy Leggitt V, Thomson M, Oyoyo U, Dan Wycliffe D. Influence of common orthodontic appliances on the diagnostic quality of cranial magnetic resonance images. Am J Orthod Dentofac Orthop 2008; 134: 563–72.
31. Beau A, Bossard D, Gebeile-Chauty S. Magnetic resonance imaging artefacts and fixed orthodontic attachements. Eur J Orthod 2015; 37: 105-10.
32. Hasegawa M, Miyata K, Abe Y, Ishigami T. Radiofrequency heating of metallic dental devices durig 3.0 T MRI. Dentomaxillofac Radiol 2013; 42: 20120234. doi: 10.1259/dmfr.20120234. Epub 2013 Mar 21.
33. Gorgulu S, Ayyıldız S, Kamburoglu K, Gokçe S, Ozen T. Effect of orthodontic brackets and different wires on radiofrequency heating and magnetic field interactions during 3-T MRI. Dentomaxillofac Radiol 2014; 43: 20130356. doi: 10.1259/dmfr.20130356. Epub 2013 Nov 20.
34. Zachriat C, Asbach P, Blankenstein K I, Peroz I, Blankenstein FH. MRI with intraoral orthodontic appliance: a comparative in vitro and in vivo study of image artefacts at 1.5 T. Dentomaxillofac Radiol 2015; 44: 20140416. doi: 10.1259/dmfr.20140416. Epub 2015 Mar 3.
35. Wylezinska M, Pinkstone M, Hay N, Scott AD, Birch MJ, Miquel ME. Impact of orthodontic appliances on the quality of craniofacial anatomical magnetic resonance imaging and real-time speech imaging. Eur J Orthod 2015; 37: 610-7.
36. Ho ML, Campeau NG, Ngo TD, Udayasankar UK, Welker KM. Pediatric brain MRI part I: basic techniques. Pediatr Radiol 2017; 47: 534-43.

Yazışma Adresi
Dr. Mehmet Hakan KURT, Assoc. Prof.,
Department of Dentomaxillofacial Radiology,
Faculty of Dentistry, Ankara University, Ankara,
06500, Turkey
Tel: 00 90 312 296 56 34
Pbx Number: 00 90 312 212 39 54
E-mail address: mhakankurt@yahoo.com